



OPEN ACCESS

EDITED BY

Alexandra Latini,
Federal University of Santa Catarina,
Brazil

REVIEWED BY

Daniele Bani,
University of Florence, Italy
Rozangela Curi Pedrosa,
Federal University of Santa Catarina,
Brazil

*CORRESPONDENCE

Joochan Woo,
✉ lsjoochan@gmail.com
Yohan Seo,
✉ ddukdae12@gmail.com,
✉ yohanseo@kmedihub.re.kr

RECEIVED 11 February 2023

ACCEPTED 19 April 2023

PUBLISHED 18 May 2023

CITATION

Park S, Das R, Nhiem NX, Jeong SB,
Kim M, Kim D, Oh HI, Cho S-H,
Kwon O-B, Choi J-H, Park CS, Kim S-R,
Moon UY, Cha B, Choi DK, Lee S,
Namkung W, Woo J and Seo Y (2023),
ANO1-downregulation induced by
schisandrathera D: a novel therapeutic
target for the treatment of prostate and
oral cancers.
Front. Pharmacol. 14:1163970.
doi: 10.3389/fphar.2023.1163970

COPYRIGHT

© 2023 Park, Das, Nhiem, Jeong, Kim,
Kim, Oh, Cho, Kwon, Choi, Park, Kim,
Moon, Cha, Choi, Lee, Namkung, Woo
and Seo. This is an open-access article
distributed under the terms of the
[Creative Commons Attribution License
\(CC BY\)](https://creativecommons.org/licenses/by/4.0/). The use, distribution or
reproduction in other forums is
permitted, provided the original author(s)
and the copyright owner(s) are credited
and that the original publication in this
journal is cited, in accordance with
accepted academic practice. No use,
distribution or reproduction is permitted
which does not comply with these terms.

ANO1-downregulation induced by schisandrathera D: a novel therapeutic target for the treatment of prostate and oral cancers

SeonJu Park¹, Raju Das², Nguyen Xuan Nhiem^{3,4},
Sung Baek Jeong⁵, Minuk Kim⁶, Dongguk Kim⁶, Hye In Oh⁷,
Su-Hyeon Cho¹, Oh-Bin Kwon⁵, Jae-Hyeog Choi⁵,
Chul Soon Park⁸, Song-Rae Kim¹, Uk Yeol Moon⁵, Boksik Cha⁵,
Dong Kyu Choi⁵, Sungwoo Lee⁵, Wan Namkung⁹,
Joochan Woo^{2,10*} and Yohan Seo^{5*}

¹Chuncheon Center, Korea Basic Science Institute, Chuncheon, Republic of Korea, ²Department of Physiology, Dongguk University College of Medicine, Gyeongju, Republic of Korea, ³Institute of Marine and Biochemistry, Vietnam Academy of Science and Technology (VAST), Hanoi, Vietnam, ⁴Graduate University of Science and Technology, Hanoi, Vietnam, ⁵New Drug Development Center, Daegu Gyeongbuk Medical Innovation Foundation, Daegu, Republic of Korea, ⁶Department of Medical Device Development Center, Daegu-Gyeongbuk Medical Innovation Foundation (KMEDI hub), Daegu, Republic of Korea, ⁷Underwood Division Economics, Underwood International College, Yonsei University, Seoul, Republic of Korea, ⁸Department of Bio-nanomaterials, Bio Campus of Korea Polytechnics, Nonsan, Republic of Korea, ⁹College of Pharmacy, Yonsei Institute of Pharmaceutical Science, Yonsei University, Incheon, Republic of Korea, ¹⁰Channelopathy Research Center (CRC), Dongguk University College of Medicine, Goyang, Republic of Korea

Anoctamin 1 (ANO1), a drug target for various cancers, including prostate and oral cancers, is an intracellular calcium-activated chloride ion channel that plays various physiopathological roles, especially in the induction of cancer growth and metastasis. In this study, we tested a novel compound isolated from *Schisandra sphenanthera*, known as schisandrathera D, for its inhibitory effect on ANO1. Schisandrathera D dose-dependently suppressed the ANO1 activation-mediated decrease in fluorescence of yellow fluorescent protein; however, it did not affect the adenosine triphosphate-induced increase in the intracellular calcium concentration or forskolin-induced cystic fibrosis transmembrane conductance regulator activity. Specifically, schisandrathera D gradually decreased the levels of ANO1 protein and significantly reduced the cell viability in ANO1-expressing cells when compared to those in ANO1-knockout cells. These effects could be attributed to the fact that schisandrathera D displayed better binding capacity to ANO1 protein than the previously known ANO1 inhibitor, Ani9. Finally, schisandrathera D increased the levels of caspase-3 and cleaved poly (ADP-ribose) polymerase 1, thereby indicating that its anticancer effect is mediated through apoptosis. Thus, this study highlights that schisandrathera D, which reduces ANO1 protein levels, has

Abbreviations: ANO1, anoctamin 1; BSA, bovine serum albumin; CFTR, cystic fibrosis transmembrane conductance regulator; FRT, Fisher rat thyroid; KO, knock-out; MM-GBSA, molecular mechanics-generalized 396 Born surface area; TMEM16A, transmembrane protein 16A; YFP, yellow fluorescent protein.

apoptosis-mediated anticancer effects in prostate and oral cancers, and thus, can be further developed into an anticancer agent.

KEYWORDS

anoctamin 1, *Schisandra sphenanthera*, oral cancer, prostate cancer, protein reduction, apoptosis

1 Introduction

Prostate cancer is characterized by the expression of androgen receptors and prostate-specific antigen markers that have a considerable impact on its development. Therefore, hormone therapies for prostate cancer often target these markers (McAllister et al., 2020). However, patients with prostatic small-cell neuroendocrine carcinoma frequently face restrictions in terms of their treatment, including hormone therapy (Butler and Huang, 2021), since androgen receptors and prostate-specific antigen markers are not expressed in this type of cancer. Likewise, oral cancer is the sixth most common cancer in the world (Liu et al., 2012a). The appropriate treatment for oral cancer constitutes radical surgery combined with radiation therapy and chemotherapy for progressive cancer, along with new and improved treatment methods such as 5-aminolevulinic acid photodynamic therapy. Despite these options, there is still a dire need for the discovery of new targets and therapeutic agents for the treatment of oral cancer (Karakullukcu et al., 2011). Thus, there is a need for the identification of a new target that can inhibit the development of these cancers (Tai et al., 2011; Lee et al., 2018).

Recently, it was revealed that anoctamin1 (ANO1) plays various role in cancer progression including prostate and oral cancers, and pharmacological inhibitors of ANO1 have been discovered (Seo et al., 2016; Seo et al., 2018; Galiotta, 2022; Jeong et al., 2022). ANO1, which has recently emerged as a drug target, is a calcium-activated chloride channel that performs various physiological functions. The use of a pharmacological inhibitor of ANO1 in prostate PC-3 cells resulted in an anticancer effect by inducing apoptosis through the increased expression of tumor necrosis factor- α (Song et al., 2018). ANO1 inhibitors were applied on prostate cancer cells and significant antiproliferative effects were observed (Seo et al., 2017; Kim et al., 2020; Jeon et al., 2023). However, a variety of compounds act on ANO1 with only limited selectivity which poses a great challenge for the validation of ANO1 as a therapeutic target (Truong et al., 2017). Techniques for targeting specific proteins based on their structure and for understanding diverse functions of membrane proteins are flourishing astonishingly. The optimal chemical compound for targeting ANO1 can be identified using the recently discovered cryogenic electron microscopy structure of ANO1 available in the Protein Data Bank (PDB) (Paulino et al., 2017); however, many of the properties of such compounds (for example, efficacy, selectivity, and safety) need to be tested (Liu et al., 2021).

The genus *Schisandra* (Schisandraceae), a twining shrub distributed throughout Asia and North America, comprises approximately 25–30 accepted species worldwide. Dibenzocyclooctadiene lignans and nortriterpenoids are the main chemical components of this genus (Li et al., 2003; Luo et al., 2012; Li et al., 2013; Shi et al., 2015). Previous phytochemical studies on *Schisandra sphenanthera*

have resulted in the identification of diverse chemical structures, including highly oxygenated nortriterpenoids, diaryldimethylbutane, dibenzocyclooctadiene lignans, and neolignans (Peng et al., 2019; Mai et al., 2021). Interestingly, the *Schisandra* lignans mentioned above demonstrate a wide range of pharmacological activities, such as cytotoxic, hepatoprotective, neuroprotective, and cognitive-enhancement (Wang et al., 2008; Li et al., 2013; Jiang et al., 2015; Sowndhararajan et al., 2018; Mai et al., 2021).

In the present study, we investigated the possible medicinal effects of phytochemicals obtained from *S. sphenanthera* occurring owing to the inhibition of ANO1, and the physiological effects of schisandrathera D on prostate and oral cancer cells. Through these investigations, we aimed to demonstrate the anticancer effects of this compound.

2 Materials and methods

2.1 Plant material

The leaves of *S. sphenanthera* Rehder & E. H. Wilson were collected from the Kon Tum province in February 2017 and identified by Dr. Nguyen, The Cuong, Institute of Ecology and Biological Resources. A voucher specimen (NCCT-P78) was deposited at the Institute of Marine Biochemistry in Vietnam.

2.2 Extraction and isolation

The dried powdered *S. sphenanthera* (5 kg) was extracted thrice with methanol (MeOH; 10 L each time), in an ultrasonic bath, at room temperature. Removal of the solvent under vacuum evaporation resulted in 220 g of crude MeOH extract (4.4% yield), which was suspended in water and partitioned with dichloromethane and then ethyl acetate, resulting in 22.3 g dichloromethane (0.4% yield), 70.0 g ethyl acetate (1.4% yield), and 89.0 g of a water layer (1.8% yield).

The ethyl acetate crude fraction was chromatographed on a silica gel column using a stepwise gradient of hexane/ethyl acetate, to yield seven fractions, E1–E7. E1 was first purified using silica gel CC, and then eluted with hexane/ethyl acetate (5/1, v/v), to yield six fractions, E1.1–E1.6. E1.2 was further purified using preparative high-performance liquid chromatography (HPLC) and as an eluent, MeOH/water (4/1, v/v) to yield schisandrathera D (3.5 mg) (Mai et al., 2021).

2.2 Cell culture

Fisher rat thyroid (FRT) cells stably expressing ANO1 and cystic fibrosis transmembrane conductance regulator (CFTR) were kindly

provided by Dr. Alan Verkman (University of California, San Francisco, CA, United States) and cultured in Coon's modified F12 medium. PC-3 (human prostate cancer cell line) and CAL-27 (human oral adenosquamous carcinoma cell line) cells were cultured in Roswell Park Memorial Institute-1640 (RPMI 1640) or Dulbecco's modified Eagle's medium. All the media contained 10% fetal bovine serum, 2 mM L-glutamine, 100 U·mL⁻¹ penicillin, and 100 µg mL⁻¹ streptomycin.

2.4 Construction of ANO1-knockout (KO) cells

The PLentiCRISPRv2 vector containing Cas9 and CRISPR guide RNA targeting ANO1 (CCTGATGCCGAGTGCAAGTA) (clone ID: X35909) was purchased from Genscript (Piscataway, NJ, United States). In total, 1,500 ng of CRISPR plasmid, 1,200 ng of packaging plasmid (psPAX2), and 400 ng of envelope plasmid (pMD2.G) were co-transfected into HEK293T cells cultured in 6-well plates. The supernatant containing lentiviral particles was collected 48 h post-transfection and filtered using a 0.45 µm syringe filter. The cells were treated overnight with lentiviral particles mixed with fresh medium at a ratio of 1:1, in 24-well plates. The ANO1-KO cells were then selected using puromycin (Sigma-Aldrich, St. Louis, MO, United States), 72 h after virus transduction.

2.5 Yellow fluorescent protein (YFP) fluorescence quenching analysis

FRT cells stably expressing both the YFP variant (YFP-H148Q/I152L/F46 L) and ANO1 were plated into 96-well plates, at a density of 2×10^3 cells per well. After 48 h of incubation, the cells in each well were washed twice with phosphate-buffered saline (PBS), following which they were incubated for 10 min with the test compounds dissolved in PBS. The YFP fluorescence in each well was measured every 0.4 s for 5 s, using the FLUO star[®] Omega microplate reader (BMG Labtech). ANO1 acts as an iodide as well as a chloride channel. ANO1 activation causes iodide influx. To measure ANO1-mediated iodide influx, 100 µL of 70 mM iodide solution with 100 µM ATP was injected into each well, 1 s after initiation of measurement. The inhibitory effect of the test compounds on ANO1 activity was measured in terms of the initial iodide influx rate, which was determined from the initial slope of the decrease in fluorescence after ATP injection.

2.6 Measurement of short-circuit currents

Snapwell[™] inserts containing ANO1- and CFTR-expressing FRT cells were mounted onto Ussing chambers (Physiologic Instruments, San Diego, CA, United States). The basolateral bath was filled with a HCO₃⁻-buffered solution containing 120 mM NaCl, 5 mM KCl, 1 mM MgCl₂, 1 mM CaCl₂, 10 mM D-glucose, 2.5 mM HEPES, and 25 mM NaHCO₃ (pH 7.4), while the apical bath was filled with a half-Cl⁻ solution. In the half-Cl⁻ solution, 65 mM NaCl

in the HCO₃⁻-buffered solution was replaced with sodium gluconate. The basolateral membrane was permeabilized with 250 µg mL⁻¹ amphotericin B. The cells were bathed for 20 min and aerated with 95% O₂/5% CO₂, at 37°C. ATP was applied to the apical membrane to activate ANO1, while forskolin was applied to the apical membrane to activate CFTR. Then, test compound was applied to both apical and basolateral bath solutions, 20 min before ANO1 and CFTR activation. Apical membrane currents were measured using an EVC4000 Multi-Channel V/I Clamp (World Precision Instruments, Sarasota, FL, United States) and PowerLab 4/35 (AD Instruments, Castle Hill, Australia). Data were analyzed using LabChart Pro 7 (AD Instruments). The sampling rate was 4 Hz.

2.7 Measurement of intracellular calcium levels

FRT cells were cultured in 96-well black-walled microplates and loaded with Fluo-4 NW, according to the manufacturer's protocol (Invitrogen, Carlsbad, CA, United States). Briefly, the cells were incubated with 100 µL assay buffer (1 × Hanks' balanced salt solution with 2.5 mM probenecid and 20 mM HEPES) containing Fluo-4 NW. After 1 h of incubation, the 96-well plates were transferred to a plate reader for the fluorescence assay. Fluo-4 fluorescence was measured using a FLUOstar[®] Omega microplate reader equipped with syringe pumps and custom Fluo-4 excitation/emission filters (485/538 nm).

2.8 Western blot analysis

Protein samples (80 µg) were separated using 4%–12% Tris-Glycine-PAG Pre-Cast Gel (Koma Biotech, South Korea) and transferred to polyvinylidene fluoride membranes. Blocking was performed using 5% bovine serum albumin (BSA) in tris-buffered saline with 0.1% Tween 20 for 1 h. The membranes were then incubated with the corresponding primary antibodies, including anti-ANO1 (Abcam, United Kingdom) and anti-β-actin (Santa Cruz Biotechnology, United States), followed by incubation with horseradish peroxidase-conjugated anti-secondary IgG antibodies (Enzo Life Science) for 1 h. Finally, visualization was performed using the ECL Plus Western Blotting System (GE Healthcare).

2.9 Cell viability assay

MTS cell proliferation assay was performed using CellTiter 96[®] Aqueous One Solution Cell Proliferation Assay Kit (Promega). PC-3 and CAL-27 cells were cultured in 96-well plates containing a medium supplemented with 3% fetal bovine serum for 24 h. Once the cells reached approximately 20% confluence, the compounds (0.03–300 µM) or vehicle (DMSO) were added to the medium, which was replaced with a fresh medium every 24 h. After 48 h of treatment, the medium was completely removed and MTS assay was performed, as recommended in the supplier's protocol. The absorbance of

formazan was measured at a wavelength of 490 nm, using an Infinite M200 microplate reader (Tecan).

2.10 Molecular docking analysis

Before docking, ligand preparation was carried out using Schrödinger Suite 2017–1. Following that, the 3D structure of the selected ligand was drawn using the ChemDraw software, while compound Ani9 was downloaded from the PubChem database (Jeong et al., 2022). For precise three-dimensional ligand models and conformational sampling, all compounds were exposed to the LigPrep module in Schrödinger Suite while maintaining a pH of 7.0 ± 2.0 for structure refinement, proper chiral formation, and ionization prediction. The entire system was run under the OPLS3 force field, with the implementation of the Epik algorithm script (version 4.4) (Shelley et al., 2007). For each ligand, a total of 32 possible stereoisomers were set. Here, the protein preparation wizard of Schrödinger suite was used to prepare the structure before docking. Due to the absence of a human crystallographic structure, we selected two cryogenic structures (PDB: 5OYB, 6BGJ), which correspond to *Mus Musculus*. Both structures were passed through the optimization and minimization steps. Additionally, proper hydrogen additions, bond order correction, and deletion of water molecules were confirmed during the preparation. After that, grid generation of the protein-ligand-binding site was also defined by following the glide-grid generation protocol in the Schrödinger Suite. For the preliminary quest of receptor-ligand-binding insights and selection of an accurate binding pose, extra precision (XP) docking was carried out to obtain a more reliable score than that obtained using standard precision (SP) docking, wherein ligands were allowed to move flexibly into the binding core (Halgren et al., 2004). As indicated by the methodology, the candidate proteins were docked with two selected ligands following the constraint minimization process. Before docking, Van der Waals scaling factor and charge cutoff were kept constant at 0.80 and 0.15, respectively, to soften the potential for nonpolar parts of the ligand. After the final docking, the lowest scores based on the best orientations were sorted for further study.

2.11 Prime molecular mechanics—generalized born surface area (MM-GBSA)

To evaluate the actual binding free energy of the complexes generated upon the docking simulation, the complexes were subjected to MM-GBSA analysis, a mixed methodology of the prime MM-GBSA protocol. MM-GBSA is a combined protocol wherein the OPLS3 force field is used to predict the molecular mechanics energy and the surface-generalized Born solvation model is used for polar solvation calculations. A non-polar solvation term composed of a non-polar solvent-accessible surface area and van der Waals interactions also constitutes a part of the total MM-GBSA calculation process (Vijayakumar et al., 2011). After the post-energy calculation, the best hits were identified as those with higher negative energy values. The

total free energy of binding was calculated using the following equation: $\Delta G_{\text{bind}} = G_{\text{complex}} - (G_{\text{protein}} + G_{\text{ligand}})$, where G = molecular mechanics energy + GSGB + non-polar solvation term.

2.12 Caspase-3 activity assay

PC-3 and CAL-27 cells were cultured in 96-well plates until they reached 30% confluence. Next, test compounds (0, 10, and 30 μM), Ac-DEVD-CHO (10 μM), a caspase-3 inhibitor, and Ani9 (10 μM) were added to the corresponding wells. After 24 h, each well was washed with PBS and incubated at room temperature with 100 μL PBS containing 1 μM NucView[®] 488 caspase-3 substrate. After 30 min of incubation, the cells were stained with 1 μM Hoechst 33342. The fluorescence of NucView[®] 488 and Hoechst 33342 was measured using a FLUOstar[®] Omega microplate reader and multicolored images were documented using a Lionheart FX Automated Microscope (BioTek, Winooski, VT, United States).

2.13 Human cleaved PARP-1 activity assay

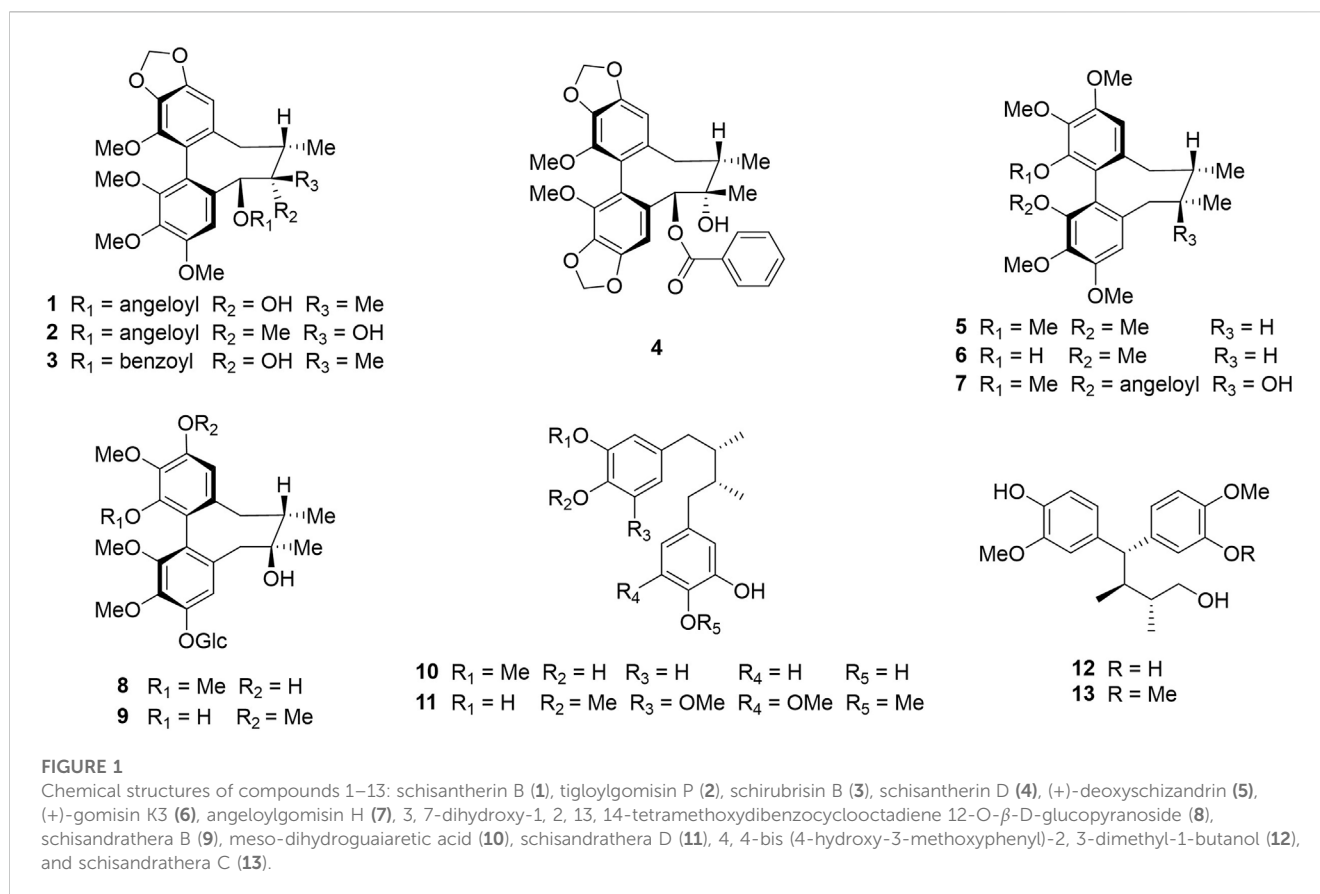
Human cleaved PARP-1 activity assay was performed according to the manufacturer's instructions (#ab174441, Abcam, United Kingdom). PC-3 and CAL-27 cells were cultured in 6-well plates until they reached 80% confluence. Test compounds were added for 24 h and 5×10^7 cells were lysed using the cell extraction buffer for 20 min. Supernatants were collected after the cells were centrifuged (13,000 rpm) for 20 min at 4°C. Next, 100 μg protein/50 μL buffer was added to each well with an antibody cocktail containing a capture antibody and detector antibody and incubated for 1 h. The wells were washed twice with 1 x wash buffer and then TMB development solution was added for 10 min. Finally, the stop solution was added, and optical density (O.D.) was measured at 450 nm using a microplate reader (Synergy[™] Neo, BioTek).

2.14 Cell-cycle analysis

PC-3 cells were seeded 2×10^5 cells/well in 100-phi culture plates and treated with the test compound for 24 h. Cells were fixed with cold 70% ethanol and incubated for 2 h at -20°C . Ethanol was removed and the cells were re-suspended in propidium iodide/Triton X-100/DNase-free RNase A staining solution for 30 min. The cell-cycle distribution was analyzed using Gallios (Beckman Coulter). A total of 2×10^3 cells per group were analyzed.

2.15 Statistical analysis

All experiments were conducted independently at least thrice. The results for the multiple trials have been presented as mean \pm standard error. Statistical analysis was performed using Student's t-test or analysis of variance, as appropriate. Statistical significance was set to $p < 0.05$. Prism software (GraphPad) was used to plot the dose-response curve and calculate the IC_{50} values.



3 Results

3.1 Identification of compounds from *S. sphenanthera*

In previous studies, we isolated thirteen dibenzocyclooctadiene lignans and neolignans, namely schisantherin B (McAllister et al., 2020), tigloylgomisin P (Butler and Huang, 2021), schirubrisin B (Lee et al., 2018), schisantherin D (Tai et al., 2011), (+)-deoxyschizandrin (Liu et al., 2012b), (+)-gomisin K3 (Karakullukcu et al., 2011), angeloylgomisin H (Sung et al., 2021), 3, 7-dihydroxy-1, 2, 13, 14-tetramethoxydibenzocyclooctadiene 12-O-β-D-glucopyranoside (Vitório et al., 2020), schisandrathera B (Jeong et al., 2022), meso-dihydroguaiaretic acid (Galietta, 2022), schisandrathera D (Seo et al., 2018), 4,4-bis(4-hydroxy-3-methoxyphenyl)-2,3-dimethyl-1-butanol (Seo et al., 2016), and schisandrathera C (Song et al., 2018), from the leaves of *S. sphenanthera* (Figure 1). Their chemical structures, including absolute configurations were determined extensively by HR-ESI-MS, NMR, and ECD spectra and comparing their NMR data with that in reported literature (Mai et al., 2021).

3.2 Cell-based high-throughput screening (HTS) for the identification of a novel natural compound that inhibits ANO1 channel

The effect of substances extracted from schisantherin on inhibiting ANO1 was measured using a cell-based screening

system. As shown in Figure 2, upon treatment with adenosine triphosphate (ATP), there is an increase in the levels of intracellular calcium, which leads to the flow of iodine into the cell through ANO1 channel activation because ANO1 channel also acts as an iodide channel. The intracellular iodine binds to the mutant YFP and strongly reduces its fluorescence. However, if an ANO1 inhibitor inhibits the ANO1 channel and blocks the influx of iodine, there is no decrease in the YFP fluorescence (Figure 2A). Upon screening of the substances isolated from schisantherin for their ANO1-inhibitory effect, schisandrathera D was found to have the strongest effect (Figure 2B).

3.3 Schisandrathera D is a selective ANO1 inhibitor

As shown in Figure 3, to check whether the inhibition of the ANO1 channel function by schisandrathera D is selective, FRT cells expressing ANO1 and YFP at different concentrations were treated with schisandrathera D for 20 min. Then, the treatment with ATP and iodide induced a decrease in the measured YFP fluorescence. Schisandrathera D inhibited the function of ANO1 in a concentration-dependent manner, with an IC₅₀ of 5.24 μM (Figures 3A, B). In addition, to determine whether schisandrathera D inhibits the CFTR chloride channel, CFTR-expressing FRT cells were differentiated for 6 days, and the short-circuit currents were measured using an Ussing chamber. When cells are treated with forskolin, an adenylyl cyclase activator, there is an increase in

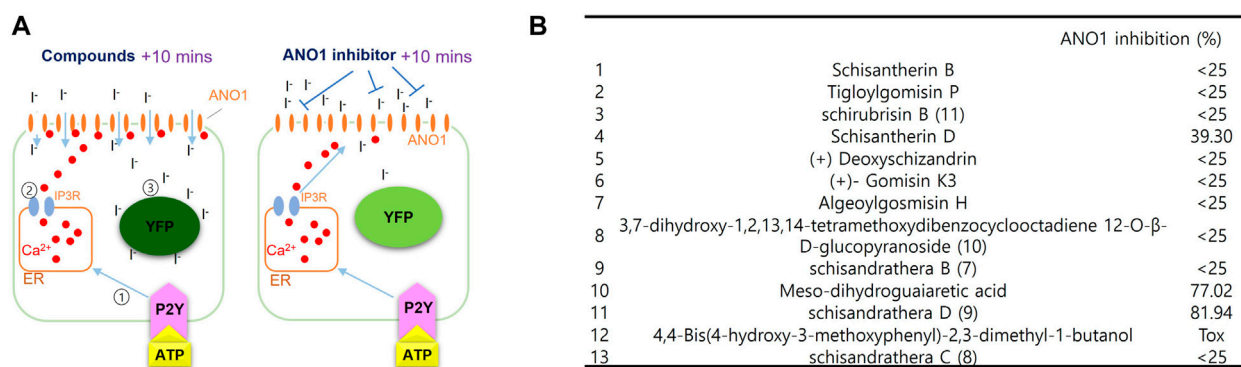


FIGURE 2 Identification of schisandrathera D using yellow fluorescent protein (YFP)-based high-throughput screening (A) A schematic representation of the cell-based YFP-reduction assay. Activation of ATP-induced P2Y receptor increases calcium levels, thereby causing activation of ANO1 channel, resulting in an influx of iodide, which quenches YFP. (B) Effects of the compounds given in the table (each used at a concentration of 10 μM) on ANO1 were assessed in terms of YFP fluorescence. The results have been presented as mean ± standard deviation (n = 5).

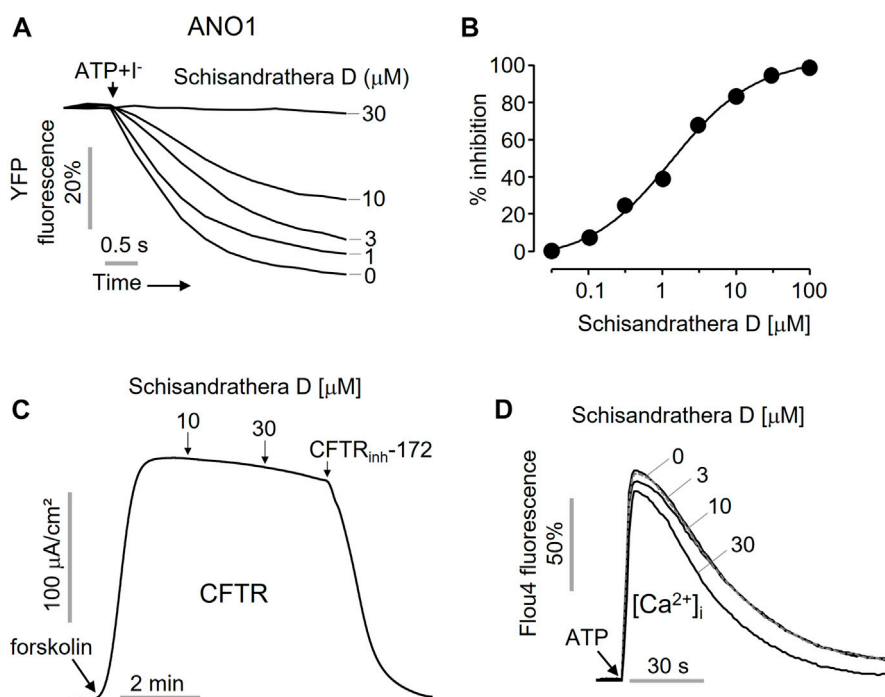
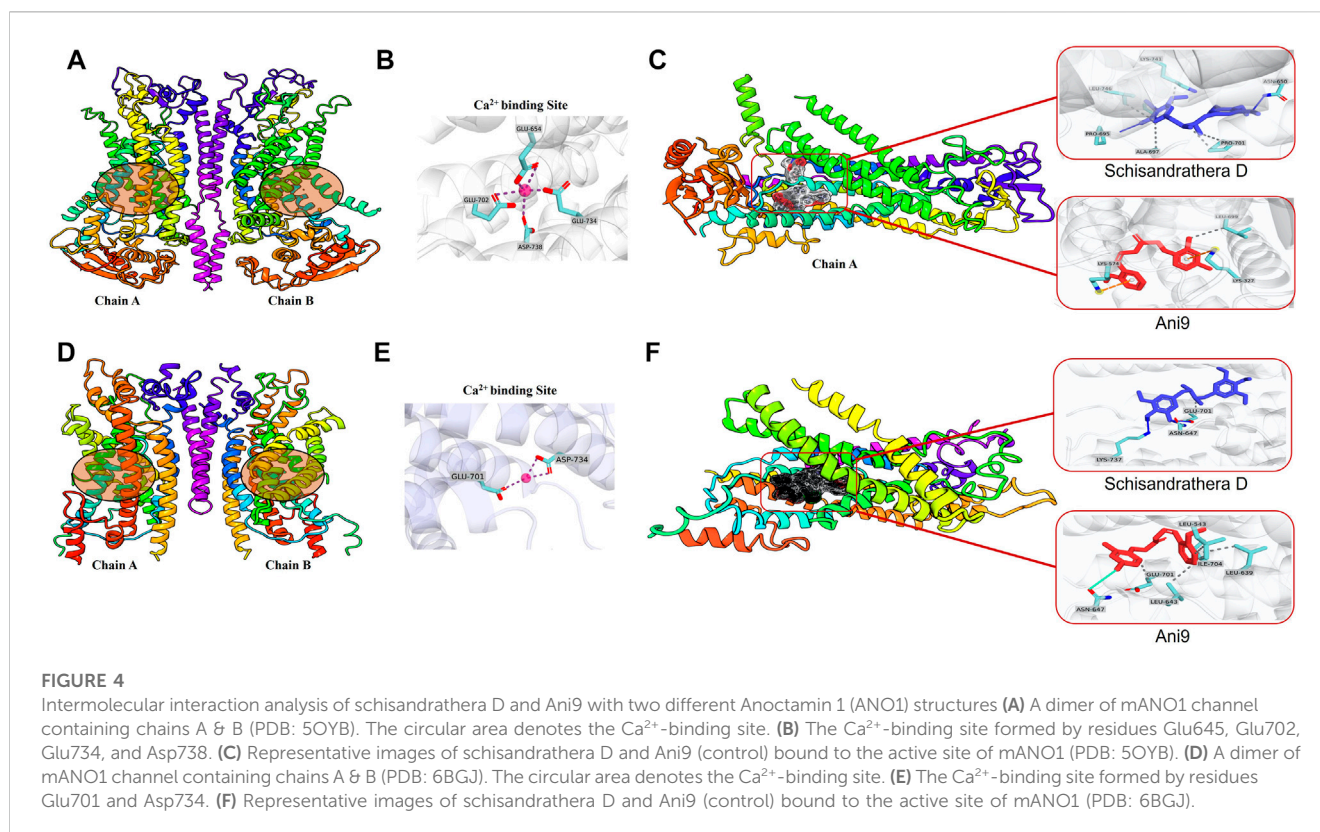


FIGURE 3 Characterization of the novel ANO1 inhibitor, schisandrathera D (A) Effects of the indicated concentrations of schisandrathera D on yellow fluorescent protein (YFP) fluorescence, upon 10-min treatment (B) Schisandrathera D inhibited Anoctamin 1 in a dose-dependent manner. (C) Effect of schisandrathera D on forskolin-induced cystic fibrosis transmembrane conductance regulator channel activity. (D) The intracellular calcium levels in Fisher rat thyroid (FRT) cells treated with schisandrathera D, as measured using Fluo-4 NW assay kit. The results have been represented as a representative trace (mean ± standard error, n = 5).

intracellular cyclic adenosine monophosphate levels, which in turn causes protein kinase A to activate CFTR. As shown in Figure 3C, schisandrathera D did not inhibit forskolin-induced CFTR activity, whereas CFTR_{inh}172, a selective CFTR inhibitor, inhibited CFTR-induced current. Since ANO1 is also activated by low calcium levels

(Arreola et al., 2022), we confirmed whether schisandrathera D had an effect on the ATP-mediated increase in intracellular calcium signaling. Since schisandrathera D had no effect on intracellular calcium levels at concentrations of up to 30 μM, it can be argued that schisandrathera D selectively inhibits ANO1.



3.4 Prediction of binding sites on the ANO1 protein

ANO1 channels are opened by voltage-dependent or voltage-gated calcium channels, and the secretion of chloride ions by ANO1 is highly dependent on calcium levels (Segura-Covarrubias et al., 2020). There are several calcium-binding sites, and when calcium is attached to its transmembrane site, the channel becomes depolarized, thereby leading to opening of pores (Ji et al., 2021). In the present study, we performed molecular docking to determine whether schisandrathera D acts at a location similar to the binding site of calcium. Glide XP docking was performed to check the molecular interaction and binding affinity, and to investigate the structure of the protein-ligand complexes after docking. Two cryogenic electron microscopy structures (PDB IDs: 5OYB and 6BGJ) were used to identify intermolecular interactions with the selected ligand after molecular docking. To date, the exact ligand-binding mechanism of ANO1 is unknown. Therefore, according to a previous study based on mutagenesis studies, putative residues involved in calcium-binding were considered as ligand-binding sites in this study (Vijayakumar et al., 2011).

Binding of the two ligands to the ANO1 binding core is shown in Figure 4 and the supplementary file (Supplementary Table S1). The docking results showed that schisandrathera D generated numerous hydrogen and hydrophobic contacts (Figures 4A–C). Schisandrathera D established hydrogen bonds with His650, His661, and His695 and interacted hydrophobically with Ala697, Pro701, Lys741, and Leu746. Ani9, however, formed a hydrophobic interaction with residue Leu699 and a π stacking interaction with Lys327 and Lys574. In contrast, schisandrathera D showed fewer

hydrogen and hydrophobic interactions with the other structure (Figures 4D–F). As shown in Figure 4F, schisandrathera D formed hydrogen bonds with Asn647, Glu701, and Lys737 in this case, and a hydrophobic contact with Glu701. Ani9 formed five hydrophobic interactions with the residues Lue543, Lue639, Lue643, Glu701, and Ile704, and a halogen contact with the residue Asn647. Based on the above interaction, the molecular docking and MM-GBSA scores of schisandrathera D with the two distinct structures suggested better binding mechanisms than those of the control, Ani9. The molecular docking and MM-GBSA scores are provided in the supplementary file (Supplementary Table S2).

3.5 Schisandrathera D reduces ANO1 protein levels and cell viability

Pharmacological inhibition of ANO1 inhibits the growth of various cancer cell types. To determine whether schisandrathera D inhibits the growth of prostate and oral cancers through a decrease in ANO1 protein levels, PC-3 and CAL-27 cells were treated with schisandrathera D and the change in the level of ANO1 protein was measured. Schisandrathera D strongly decreased the ANO1 protein levels in both cell lines (Figures 5A, B). In addition, we also generated ANO1-KO cells using CRISPR-Cas9 system. These genetically engineered cells were also treated with different concentrations of schisandrathera D, following which cell viability was measured. Schisandrathera D decreased cell viability in a concentration-dependent manner in cells with high ANO1 levels, but there was no such inhibitory effect in ANO1-KO cells (Figures 5C, D).

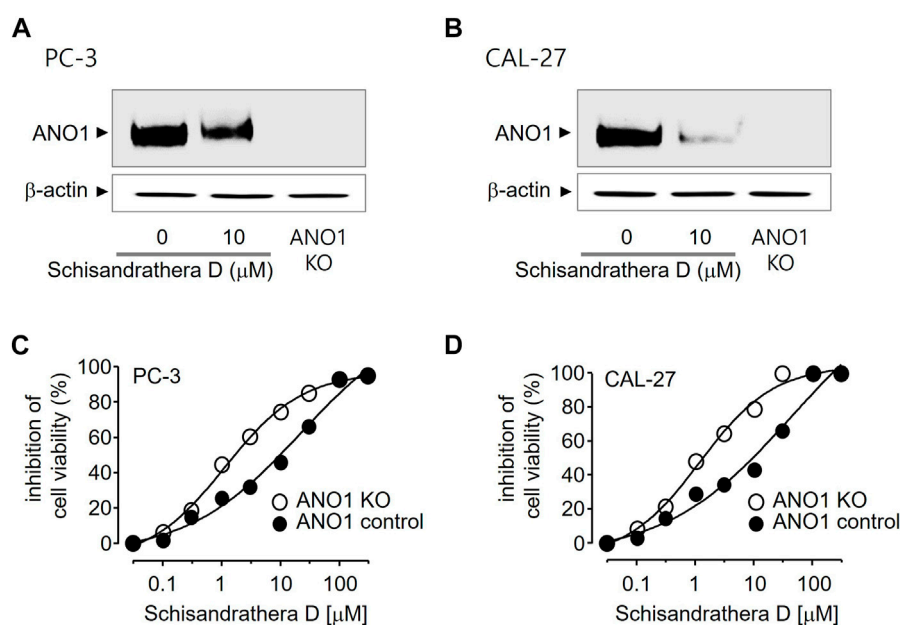


FIGURE 5

Effects of schisandrathera D on Anoctamin 1 (ANO1) protein expression and cell viability (A,B) PC-3 and CAL-27 cells were cultured with 10 μM schisandrathera D for 24 h. ANO1 expression in PC-3/CAL-27 ANO1-KO cells. The loading control was β-actin. (C,D) Effects of the indicated concentrations of schisandrathera D on cell viability of PC-3 or PC-3 ANO1-KO cells and CAL-27 or CAL-27 ANO1-KO cells. The data have been represented as mean ± standard deviation ($n = 5$).

3.6 Assessment of the apoptotic effect of schisandrathera D

Reduction or pharmacological inhibition of ANO1 induces apoptosis. We treated PC-3 and CAL-27 cells expressing high levels of ANO1 with schisandrathera D and determined if this treatment induced apoptosis. Schisandrathera D significantly increased the activity of caspase-3 and poly (ADP-ribose) polymerase 1 cleavage, which serve as two hallmarks of apoptosis, while Ani9 did not increase the latter (Figure 6). Although Ani9 is a known ANO1 inhibitor, its effect on reducing the ANO1 protein levels was weak. Schisandrathera D, however, induced an apoptotic effect and G2M arrest by strongly decreasing the ANO1 protein levels.

4 Discussion

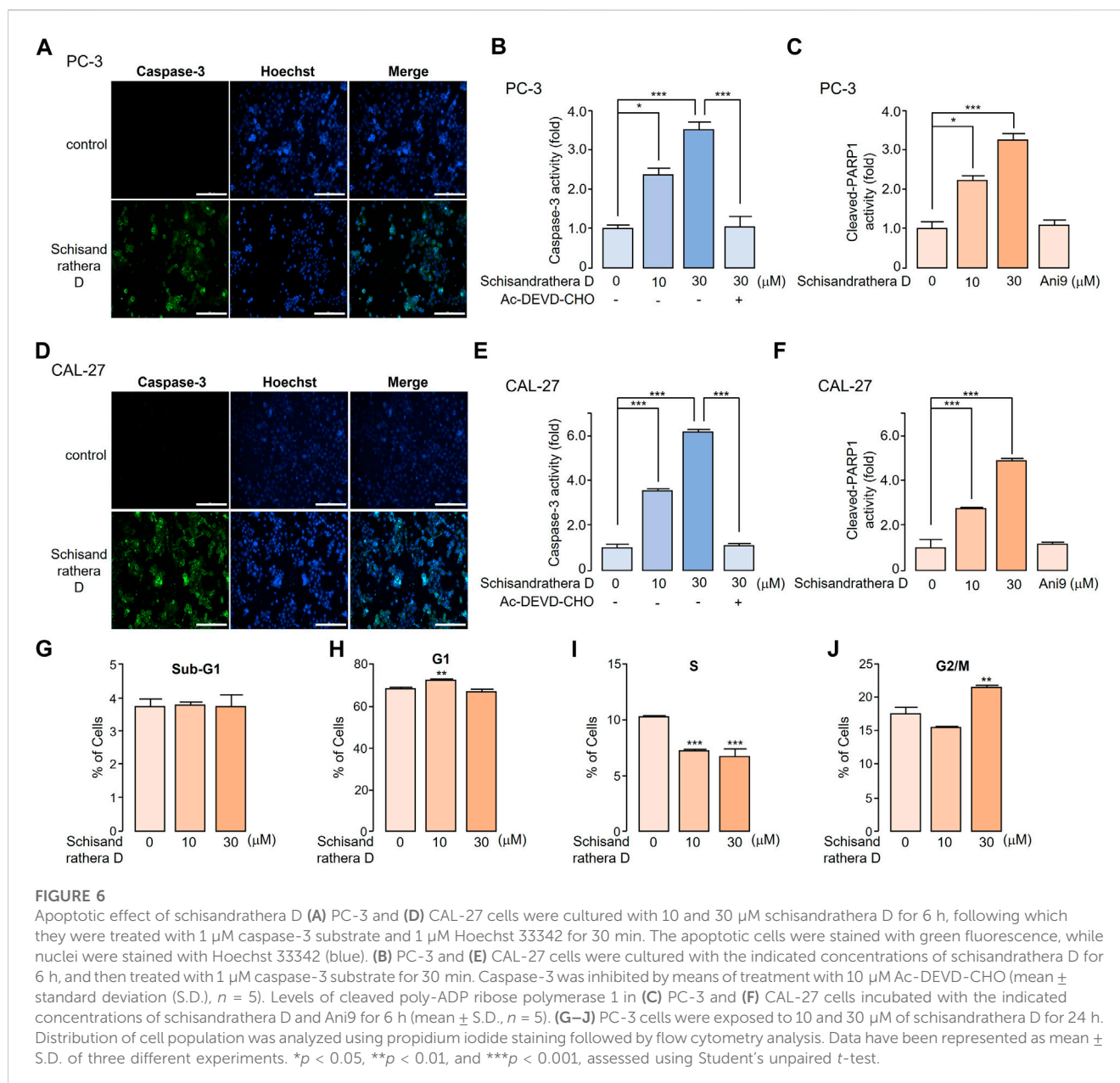
Although the physiological functions of ANO1 are diverse and include secretion of chloride ions and the development of cancer (Hwang et al., 2009; Cho et al., 2012; Huang et al., 2012; Ji et al., 2019), the inhibition of the function of ANO1 channel and reduction of its protein expression has therapeutic effects in head and neck cancers, and in prostate cancers (Ayoub et al., 2010; Liu et al., 2012a; Duvvuri et al., 2012). In recent studies, ANO1 has been proposed as a potential therapeutic target for several cancers, including OSCC. No molecules which can ameliorate OSCC via ANO1 inhibition are known to date (Ruiz et al., 2012; Britschgi et al., 2013; Li et al., 2014; Seo et al., 2015). Therefore, it is necessary to find novel molecules that can reduce ANO1 channel function or ANO1 protein levels. In

this study, we found that schisandrathera D reduced the ANO1 channel function in a dose-dependent manner. Interestingly, schisandrathera D neither inhibited CFTR activity, nor the ATP-induced changes in calcium levels, thereby behaving as a selective ANO1 inhibitor (Figures 2, 3).

To date, several ANO1 inhibitors have been developed (Galiotta et al., 2001; Namkung et al., 2010; Seo et al., 2016; Seo et al., 2018). Therefore, several research groups tried to develop specific ANO1 inhibitors, starting from hit to lead chemical compounds via lead optimization (Seo et al., 2018; Wang et al., 2022). However, they have not reached clinical trials because they generally have low *in vitro* stability and *in vivo* efficacy (Choi et al., 2021; Wang et al., 2021; Zhang et al., 2021).

Therefore, natural products may provide a breakthrough in this field of research, being effective ANO1 inhibitors; furthermore, such products may be safer. Thus, many researchers are actively conducting studies to develop anticancer drugs based on natural products (Kim and Kim, 2018; Spradlin et al., 2019).

We have demonstrated for the first time that the natural compound schisandrathera D, isolated from the leaves of *S. sphenanthera*, strongly inhibits the function of ANO1 channels by binding to the ANO1 protein site (Figure 4). Schisandrathera D appears to bind to a specific region of the ANO1 protein with high absolute binding free energy and prevent its activation by calcium (Tai et al., 2011). Furthermore, there appears to be a high probability that this binding to ANO1 is beneficial for reducing its protein levels. Ani9 binds to ANO1 protein with low binding free energy, but does not reduce the ANO1 protein levels (Seo et al., 2021). However, since ANO1 activation can be caused by several molecular factors such as internal levels of calcium, calcium binding protein (CaM) and



inositol triphosphate (Hawn et al., 2021), the mechanism underlying the schisandrathera D-mediated reduction in protein levels requires further study.

Schisandrathera D seems to be an effective anticancer therapeutic option, acting through ANO1 inhibition. Treatment of PC-3 and CAL-27 cells with dose-dependent concentrations of schisandrathera D reduced their viability; however, this ANO1-dependent reduction in cell viability was more marked in PC-3 and CAL-27 cells that expressed high levels of ANO1. However, schisandrathera D did inhibit cell viability weakly in ANO1 KO-PC-3 and -CAL-27 cells. This suggests that the anticancer mechanism of schisandrathera D is, at least partly, mediated by the reduction of ANO1 expression. Moreover, Ani9 (the only functional ANO1 inhibitor) did not induce apoptosis. Similarly, luteolin, an ANO1 inhibitor, displays anticancer effects through the downregulation of ANO1 in cancer cells (Seo et al.,

2017). Therefore, it is possible that the downregulation of ANO1 by schisandrathera D represents an important anticancer mechanism. However, future studies should focus on the comparative assessment of the absorption and metabolic rates of natural products, such as ANO1 inhibitors schisandrathera D and luteolin.

In conclusion, schisandrathera D inhibited ANO1 channel function and decreased ANO1 protein levels. Schisandrathera D decreased the viability of prostate and oral cancer cells and exerted its anticancer effects by activating apoptosis via the reduction of ANO1 protein levels. However, the anticancer effect was insignificant in cells not expressing ANO1. Similar results were obtained for Ani9, an inhibitor of ANO1 function. Further structure-activity relationship studies should be carried out to develop safer and superior ANO1 inhibitors based on the structure of schisandrathera D. Nevertheless, the results of this

study suggest schisandrathera D as a promising lead compound for the development of oral and prostate cancer therapeutic targets which act by targeting ANO1.

Data availability statement

The original contributions presented in the study are included in the article/Supplementary Material, further inquiries can be directed to the corresponding authors.

Author contributions

SP: conceptualization, methodology, data Curation, writing—original draft preparation, project administration. RD: methodology, software. NXN: methodology. JSB: methodology. MK: formal analysis. DK: formal analysis. HIO: writing—review and editing. SHC: methodology. OBK: methodology. JHC: methodology. CSP: methodology. SRK: formal analysis. UYM: formal analysis. BC: data Curation. DC: data Curation. SL: conceptualization. WN: resources. JW: conceptualization, methodology software. YS: conceptualization, methodology, formal analysis, investigation, writing-review, editing, supervision, funding acquisition.

Funding

This work was supported by the National Research Foundation of Korea (NRF) grant funded by the Koreangovernment (NRF-2021R1F1A1060694, NRF-2022M3A9J3073020, NRF-2022M3A9J4079468, NRF-2022R1F1A1063364 and NRF-2022K2A9A1A06088842). This research was supported by a

References

- Arreola, J., Pérez-Cornejo, P., Segura-Covarrubias, G., Corral-Fernández, N., León-Aparicio, D., and Guzmán-Hernández, M. L. (2022). Function and regulation of the calcium-activated chloride channel anoctamin 1 (TMEM16A). *Handb. Exp. Pharmacol.* 2022, 592. doi:10.1007/164_2022_592
- Ayoub, C., Wasyluk, C., Li, Y., Thomas, E., Marisa, L., Robé, A., et al. (2010). ANO1 amplification and expression in HNSCC with a high propensity for future distant metastasis and its functions in HNSCC cell lines. *Br. J. Cancer.* 103, 715–726. doi:10.1038/sj.bjc.6605823
- Britschgi, A., Bill, A., Brinkhaus, H., Rothwell, C., Clay, I., Duss, S., et al. (2013). Calcium-activated chloride channel ANO1 promotes breast cancer progression by activating EGFR and CAMK signaling. *Proc. Natl. Acad. Sci. U. S. A.* 110, E1026–E1034. doi:10.1073/pnas.1217072110
- Butler, W., and Huang, J. (2021). Neuroendocrine cells of the prostate: Histology, biological functions, and molecular mechanisms. *Precis. Clin. Med.* 4, 25–34. doi:10.1093/pcmedi/pbab003
- Cho, H., Yang, Y. D., Lee, J., Lee, B., Kim, T., Jang, Y., et al. (2012). The calcium-activated chloride channel anoctamin 1 acts as a heat sensor in nociceptive neurons. *Nat. Neurosci.* 15, 1015–1021. doi:10.1038/nn.3111
- Choi, M. R., Kim, H. D., Cho, S., Jeon, S. H., Kim, D. H., Wee, J., et al. (2021). TMEM16A induces hyperproliferation of HaCaT keratinocytes and triggers imiquimod-induced psoriasis-like skin injury in mice. *Int. J. Mol. Sci.* 22, 7145. doi:10.3390/ijms22137145
- Duvvuri, U., Shiwarski, D. J., Xiao, D., Bertrand, C., Huang, X., Edinger, R. S., et al. (2012). TMEM16A induces MAPK and contributes directly to tumorigenesis and cancer progression. *Cancer Res.* 72, 3270–3281. doi:10.1158/0008-5472.CAN-12-0475-T
- Galiotta, L. J., Springsteel, M. F., Eda, M., Niedziński, E. J., By, K., Haddadin, M. J., et al. (2001). Novel CFTR chloride channel activators identified by screening of

research grant from “Creative KMEDI hub” in 2022 “(Project Name: Development of a selective ANO1 degrader that overcomes the resistance to NSCLC treatment/Project No: B-B-N-22-03)” and under the framework of Global Joint Research Promotion Program managed by the National Research Council of Science and Technology (NST, Grant No. 1711122746) of the Ministry of Science and ICT (MSIT).

Conflict of interest

Authors SBJ, O-BK, J-HC, UM, BC, DC, SL, YS, MK, and DK were employed by the Daegu Gyeongbuk Medical Innovation Foundation (KMEDI hub).

The remaining authors declare that the research was conducted in the absence of any commercial or financial relationships that could be construed as a potential conflict of interest.

Publisher's note

All claims expressed in this article are solely those of the authors and do not necessarily represent those of their affiliated organizations, or those of the publisher, the editors and the reviewers. Any product that may be evaluated in this article, or claim that may be made by its manufacturer, is not guaranteed or endorsed by the publisher.

Supplementary material

The Supplementary Material for this article can be found online at: <https://www.frontiersin.org/articles/10.3389/fphar.2023.1163970/full#supplementary-material>

combinatorial libraries based on flavone and benzoquinolinium lead compounds. *J. Biol. Chem.* 276, 19723–19728. doi:10.1074/jbc.M101892200

Galiotta, L. J. V. (2022). TMEM16A (ANO1) as a therapeutic target in cystic fibrosis. *Curr. Opin. Pharmacol.* 64, 102206. doi:10.1016/j.coph.2022.102206

Halgren, T. A., Murphy, R. B., Friesner, R. A., Beard, H. S., Frye, L. L., Pollard, W. T., et al. (2004). Glide: A new approach for rapid, accurate docking and scoring. 2. Enrichment factors in database screening. *J. Med. Chem.* 47, 1750–1759. doi:10.1021/jm030644s

Hawn, M. B., Akin, E., Hartzell, H. C., Greenwood, I. A., and Leblanc, N. (2021). Molecular mechanisms of activation and regulation of ANO1-Encoded Ca(2+)-activated Cl(−) channels. *Channels (Austin)* 15, 569–603. doi:10.1080/19336950.2021.1975411

Huang, F., Wong, X., and Jan, L. Y. (2012). International union of basic and clinical pharmacology. LXXXV: Calcium-activated chloride channels. *Pharmacol. Rev.* 64, 1–15. doi:10.1124/pr.111.005009

Hwang, S. J., Blair, P. J., Britton, F. C., O'Driscoll, K. E., Hennig, G., Bayguinov, Y. R., et al. (2009). Expression of anoctamin 1/TMEM16A by interstitial cells of Cajal is fundamental for slow wave activity in gastrointestinal muscles. *J. Physiol.* 587, 4887–4904. doi:10.1113/jphysiol.2009.176198

Jeon, D., Jo, M., Lee, Y., Park, S. H., Phan, H. T. L., Nam, J. H., et al. (2023). Inhibition of ANO1 by cis- and trans-resveratrol and their anticancer activity in human prostate cancer PC-3 cells. *Int. J. Mol. Sci.* 24, 1186. doi:10.3390/ijms24021186

Jeong, S. B., Das, R., Kim, D. H., Lee, S., Oh, H. I., Jo, S., et al. (2022). Anticancer effect of verteporfin on non-small cell lung cancer via downregulation of ANO1. *Biomed. Pharmacother.* 153, 113373. doi:10.1016/j.biopha.2022.113373

- Ji, Q., Guo, S., Wang, X., Pang, C., Zhan, Y., Chen, Y., et al. (2019). Recent advances in TMEM16A: Structure, function, and disease. *J. Cell. Physiol.* 234, 7856–7873. doi:10.1002/jcp.27865
- Ji, W., Shi, D., Shi, S., Yang, X., Chen, Y., An, H., et al. (2021). TMEM16A protein: Calcium-binding site and its activation mechanism. *Protein Pept. Lett.* 28, 1338–1348. doi:10.2174/0929866528666211105112131
- Jiang, Y., Fan, X., Wang, Y., Tan, H., Chen, P., Zeng, H., et al. (2015). Hepatoprotective effects of six *Schisandra* lignans on acetaminophen-induced liver injury are partially associated with the inhibition of CYP-mediated bioactivation. *Chem. Biol. Interact.* 231, 83–89. doi:10.1016/j.cbi.2015.02.022
- Karakullukcu, B., van Oudenaarde, K., Copper, M. P., Klop, W. M., van Veen, R., Wildeman, M., et al. (2011). Photodynamic therapy of early stage oral cavity and oropharynx neoplasms: An outcome analysis of 170 patients. *Eur. Arch. Otorhinolaryngol.* 268, 281–288. doi:10.1007/s00405-010-1361-5
- Kim, C., and Kim, B. (2018). Anti-cancer natural products and their bioactive compounds inducing ER stress-mediated apoptosis: A review. *Nutrients* 10, 1021. doi:10.3390/nu10081021
- Kim, T., Cho, S., Oh, H., Hur, J., Kim, H., Choi, Y. H., et al. (2020). Design of anticancer 2,4-diaminopyrimidines as novel anoctamin 1 (ANO1) ion channel blockers. *Molecules* 25, 5180. doi:10.3390/molecules25215180
- Lee, Y. J., Jung, O., Lee, J., Son, J., Cho, J. Y., Ryou, C., et al. (2018). Maclurin exerts anti-cancer effects on PC3 human prostate cancer cells via activation of p38 and inhibitions of JNK, FAK, AKT, and c-Myc signaling pathways. *Nutr. Res.* 58, 62–71. doi:10.1016/j.nutres.2018.07.003
- Li, R. T., Zhao, Q. S., Li, S. H., Han, Q. B., Sun, H. D., Lu, Y., et al. (2003). Micrandilactone A: A novel triterpene from *Schisandra micrantha*. *Org. Lett.* 5, 1023–1026. doi:10.1021/ol027524j
- Li, Y. F., Jiang, Y., Huang, J. F., and Yang, G. Z. (2013). Four new lignans from *Schisandra sphenanthera*. *J. Asian Nat. Prod. Res.* 15, 934–940. doi:10.1080/10286020.2013.824428
- Li, Y., Zhang, J., and Hong, S. (2014). ANO1 as a marker of oral squamous cell carcinoma and silencing ANO1 suppresses migration of human SCC-25 cells. *Med. Oral Patol. Oral Cir. Bucal.* 19, e313–e319. doi:10.4317/medoral.19076
- Liu, W., Feng, J. Q., Shen, X. M., Wang, H. Y., Liu, Y., and Zhou, Z. T. (2012a). Two stem cell markers, ATP-binding cassette, G2 subfamily (ABCG2) and BMI-1, predict the transformation of oral leukoplakia to cancer: A long-term follow-up study. *Cancer* 118, 1693–1700. doi:10.1002/cncr.26483
- Liu, W., Lu, M., Liu, B., Huang, Y., and Wang, K. (2012b). Inhibition of Ca(2+)-activated Cl(−) channel ANO1/TMEM16A expression suppresses tumor growth and invasiveness in human prostate carcinoma. *Cancer Lett.* 326, 41–51. doi:10.1016/j.canlet.2012.07.015
- Liu, Y., Liu, Z., and Wang, K. (2021). The Ca(2+)-activated chloride channel ANO1/tmem16a: An emerging therapeutic target for epithelium-originated diseases? *Acta Pharm. Sin. B* 11, 1412–1433. doi:10.1016/j.apsb.2020.12.003
- Luo, X., Shi, Y. M., Luo, R. H., Luo, S. H., Li, X. N., Wang, R. R., et al. (2012). Schilancitrilactones A-C: Three unique nortriterpenoids from *Schisandra lancifolia*. *Org. Lett.* 14, 1286–1289. doi:10.1021/ol300099e
- Mai, N. T., Doan, V. V., Lan, H. T. T., Anh, B. T. M., Hoang, N. H., Tai, B. H., et al. (2021). Chemical constituents from *Schisandra sphenanthera* and their cytotoxic activity. *Nat. Prod. Res.* 35, 3360–3369. doi:10.1080/14786419.2019.1700247
- McAllister, M., Constância, V., Patek, S., Gan, H. W. G., Bailey, P., Wheadon, H., et al. (2020). Inflammatory infiltration is associated with AR expression and poor prognosis in hormone naïve prostate cancer. *Prostate* 80, 1353–1364. doi:10.1002/pros.24064
- Namkung, W., Thiagarajah, J. R., Phuan, P. W., and Verkman, A. S. (2010). Inhibition of Ca²⁺-activated Cl[−] channels by gallotannins as a possible molecular basis for health benefits of red wine and green tea. *FASEB J.* 24, 4178–4186. doi:10.1096/fj.10-160648
- Paulino, C., Kalienkova, V., Lam, A. K. M., Neldner, Y., and Dutzler, R. (2017). Activation mechanism of the calcium-activated chloride channel TMEM16A revealed by cryo-EM. *Nature* 552, 421–425. doi:10.1038/nature24652
- Peng, W., Liu, Y., Hu, M., Zhang, M., Yang, J., Liang, F., et al. (2019). Toona sinensis: A comprehensive review on its traditional usages, phytochemistry, pharmacology and toxicology. *Rev. Bras. Farmacogn.* 29, 111–124. doi:10.1016/j.bjp.2018.07.009
- Ruiz, C., Martins, J. R., Rudin, F., Schneider, S., Dietsche, T., Fischer, C. A., et al. (2012). Enhanced expression of ANO1 in head and neck squamous cell carcinoma causes cell migration and correlates with poor prognosis. *PLOS ONE* 7, e43265. doi:10.1371/journal.pone.0043265
- Segura-Covarrubias, G., Aréchiga-Figueroa, I. A., De Jesús-Pérez, J. J., Sánchez-Solano, A., Pérez-Cornejo, P., and Arreola, J. (2020). Voltage-dependent protonation of the calcium pocket enable activation of the calcium-activated chloride channel Anoctamin-1 (TMEM16A). *Sci. Rep.* 10, 6644. doi:10.1038/s41598-020-62860-9
- Seo, Y., Jeong, S. B., Woo, J. H., Kwon, O. B., Lee, S., Oh, H. I., et al. (2021). Diethylstilbestrol, a novel ANO1 inhibitor, exerts an anticancer effect on non-small cell lung cancer via inhibition of ANO1. *Int. J. Mol. Sci.* 22, 7100. doi:10.3390/ijms22137100
- Seo, Y., Kim, J., Chang, J., Kim, S. S., Namkung, W., and Kim, I. (2018). Synthesis and biological evaluation of novel Ani9 derivatives as potent and selective ANO1 inhibitors. *Eur. J. Med. Chem.* 160, 245–255. doi:10.1016/j.ejmech.2018.10.002
- Seo, Y., Lee, H. K., Park, J., Jeon, D. K., Jo, S., Jo, M., et al. (2016). Ani9, A novel potent small-molecule ANO1 inhibitor with negligible effect on ANO2. *PLOS ONE* 11, e0155771. doi:10.1371/journal.pone.0155771
- Seo, Y., Park, J., Kim, M., Lee, H. K., Kim, J. H., Jeong, J. H., et al. (2015). Inhibition of ANO1/TMEM16A chloride channel by idebenone and its cytotoxicity to cancer cell lines. *PLOS ONE* 10, e0133656. doi:10.1371/journal.pone.0133656
- Seo, Y., Ryu, K., Park, J., Jeon, D. K., Jo, S., Lee, H. K., et al. (2017). Inhibition of ANO1 by luteolin and its cytotoxicity in human prostate cancer PC-3 cells. *PLOS ONE* 12, e0174935. doi:10.1371/journal.pone.0174935
- Shelley, J. C., Cholleti, A., Frye, L. L., Greenwood, J. R., Timlin, M. R., and Uchimaya, M. (2007). Epik: A software program for pK(a) prediction and protonation state generation for drug-like molecules. *J. Comput. Aid. Mol. Des.* 21, 681–691. doi:10.1007/s10822-007-9133-z
- Shi, Y. M., Xiao, W. L., Pu, J. X., and Sun, H. D. (2015). Triterpenoids from the schisandraceae family: An update. *Nat. Prod. Rep.* 32, 367–410. doi:10.1039/c4np00117f
- Song, Y., Gao, J., Guan, L., Chen, X., Gao, J., and Wang, K. (2018). Inhibition of ANO1/TMEM16A induces apoptosis in human prostate carcinoma cells by activating TNF-α signaling. *Cell Death Dis.* 9, 703. doi:10.1038/s41419-018-0735-2
- Sowndhararajan, K., Deepa, P., Kim, M., Park, S. J., and Kim, S. (2018). An overview of neuroprotective and cognitive enhancement properties of lignans from *Schisandra chinensis*. *Biomed. Pharmacother.* 97, 958–968. doi:10.1016/j.biopha.2017.10.145
- Spradlin, J. N., Hu, X., Ward, C. C., Brittain, S. M., Jones, M. D., Ou, L., et al. (2019). Harnessing the anti-cancer natural product nimbolide for targeted protein degradation. *Nat. Chem. Biol.* 15, 747–755. doi:10.1038/s41589-019-0304-8
- Sung, H., Ferlay, J., Siegel, R. L., Laversanne, M., Soerjomataram, I., Jemal, A., et al. (2021). Global cancer statistics 2020: GLOBOCAN estimates of incidence and mortality worldwide for 36 cancers in 185 countries. *CA Cancer J. Clin.* 71, 209–249. doi:10.3322/caac.21660
- Tai, S., Sun, Y., Squires, J. M., Zhang, H., Oh, W. K., Liang, C. Z., et al. (2011). PC3 is a cell line characteristic of prostatic small cell carcinoma. *Prostate* 71, 1668–1679. doi:10.1002/pros.21383
- Truong, E. C., Phuan, P. W., Reggi, A. L., Ferrera, L., Galiotta, L. J. V., Levy, S. E., et al. (2017). Substituted 2-Acylaminocycloalkylthiophene-3-carboxylic acid arylamides as inhibitors of the calcium-activated chloride channel transmembrane protein 16A (TMEM16A). *J. Med. Chem.* 60, 4626–4635. doi:10.1021/acs.jmedchem.7b00020
- Vijayakumar, B., Umamaheswari, A., Puratchikody, A., and Velmurugan, D. (2011). Selection of an improved HDAC8 inhibitor through structure-based drug design. *Bioinformation* 7, 134–141. doi:10.6026/97320630007134
- Vitório, J. G., Duarte-Andrade, F. F., Dos Santos Fontes Pereira, T., Fonseca, F. P., Amorim, L. S. D., Martins-Chaves, R. R., et al. (2020). Metabolic landscape of oral squamous cell carcinoma. *Metabolomics* 16, 105. doi:10.1007/s11306-020-01727-6
- Wang, B. L., Hu, J. P., Tan, W., Sheng, L., Chen, H., and Li, Y. (2008). Simultaneous quantification of four active *Schisandra* lignans from a traditional Chinese medicine *Schisandra chinensis* (Wuweizi) in rat plasma using liquid chromatography/mass spectrometry. *J. Chromatogr. B Anal. Technol. Biomed. Life Sci.* 865, 114–120. doi:10.1016/j.jchromb.2008.02.016
- Wang, Y., Gao, J., Zhao, S., Song, Y., Huang, H., Zhu, G., et al. (2021). Discovery of 4-arylthiophene-3-carboxylic acid as inhibitor of ANO1 and its effect as analgesic agent. *Acta Pharm. Sin. B* 11, 1947–1964. doi:10.1016/j.apsb.2020.11.004
- Wang, Y., Hu, X., Huang, H., Jin, Z., Gao, J., Guo, Y., et al. (2022). Optimization of 4-arylthiophene-3-carboxylic acid derivatives as inhibitors of ANO1: Lead optimization studies toward their analgesic efficacy for inflammatory pain. *Eur. J. Med. Chem.* 237, 114413. doi:10.1016/j.ejmech.2022.114413
- Zhang, X., Zhang, G., Zhao, Z., Xiu, R., Jia, J., Chen, P., et al. (2021). Cepharanthine, a novel selective ANO1 inhibitor with potential for lung adenocarcinoma therapy. *Biochim. Biophys. Acta Mol. Cell Res.* 1868, 119132. doi:10.1016/j.bbamcr.2021.119132